Observations of non-dimensional wind shear in the coastal zone

By DEAN VICKERS* and L. MAHRT
Oregon State University, USA

SUMMARY

Vertical profiles of the time-averaged wind stress, wind speed and buoyancy flux from the off-shore tower site in the Risø Air Sea Experiment are used to evaluate similarity theory in the coastal zone. The observed dependence of the non-dimensional wind shear on stability is compared to the traditional parametrization. Relationships between the non-dimensional shear, development of internal boundary layers and wave state are explored.

We find that the largest-scale turbulent eddies are suppressed in shallow convective internal boundary layers, leading to larger non-dimensional shear than that of the traditional prediction based only on stability. In shallow stable boundary layers, elevated generation of turbulence leads to smaller non-dimensional shear compared to the traditional prediction. Over young growing waves in stable stratification, the observed non-dimensional shear is less than that over older more mature waves in otherwise similar conditions. The non-dimensional shear is a function of wave state for stable conditions even though the observations are well above the wave boundary layer. We conclude that development of shallow internal boundary layers and young growing-wave fields, both of which are common in the coastal zone, can lead to substantial departures of the non-dimensional shear from the prediction based only on stability.

KEYWORDS: Boundary layer   Similarity theory   Turbulence

1. INTRODUCTION

Monin–Obukhov (MO) similarity theory predicts that for homogeneous and stationary conditions, the non-dimensional wind shear (ϕ_m) is a universal function of atmospheric stability alone, such that

$$\phi_m(z/L) = \frac{\kappa z}{u_*} \frac{\partial u}{\partial z} \qquad (1)$$

where z is height, u is velocity, z/L is the stability parameter, L is the Obukhov length (Monin and Obukhov 1954), which is a function of the friction velocity (u_*) and the buoyancy flux, and κ is von Karman's constant. MO similarity theory applies in the surface layer above the roughness sub-layer over land, and above the wave boundary layer over water (Chalikov and Makin 1991). The top of the wave boundary layer has been defined as the height above the waves where the component of the stress in phase with the waves becomes a small fraction of the total stress. This height is thought to be approximately $\lambda/10$ (Chalikov and Belevich 1993) or $\lambda/6$ (Wetzel *et al.* 1996), where λ is the wave length of the dominant surface-wave mode. For further discussion of the wave boundary layer, see Belcher and Hunt (1998), Makin *et al.* (1995) and Large *et al.* (1995). The upper boundary of the surface layer where MO similarity theory applies is determined by the assumption that the height-dependence of the fluxes must be neglected. This normally implies that the surface layer is thin compared to the boundary layer depth. Grant (1992) has suggested that MO similarity theory should be generalized in some circumstances to include the influence of additional length scales, such as the depth of the boundary layer.

In this study, coincident measurements of vertical profiles of wind speed and vertical profiles of turbulent fluxes of momentum and buoyancy, collected during the Risø Air Sea Experiment (RASEX), are used to evaluate similarity theory hypotheses in the marine surface layer. The RASEX dataset is the first dataset with detailed vertical resolution of the time-averaged structure in off-shore flow. The RASEX off-shore flow

---

* Corresponding author: College of Oceanic and Atmospheric Sciences, Oregon State University, Corvallis, OR 97331, USA.

observations provide an opportunity to study young developing wave fields and shallow internal boundary layers (IBLs). Shallow IBLs are common in the coastal zone due to the roughness and heat flux discontinuity at the land–sea boundary (Garratt 1990; Mahrt *et al.* 1998). The observed dependence of the non-dimensional shear on z/L will be compared to the traditional land-based parametrization, and relationships between the non-dimensional shear, wave state and IBL development will be explored.

2. SIMILARITY THEORY

The non-dimensional shear of MO similarity theory has typically been evaluated by measuring the turbulent fluxes at a height thought to be in the surface layer, often taken as 10 m, and the shear from the mean wind speed at 2 levels which encompass the turbulence measurements. Data collected over land in several field programmes (e.g. Businger *et al.* 1971; Dyer 1974; Högström 1988) have been used to fit empirically the functional form of $\phi_m(z/L)$. These studies have generally confirmed that the non-dimensional shear appears to be a universal function of z/L. A commonly used parametrization (Dyer 1974) based on data from these field programmes is

$$\phi_m(z/L) = \{1 - 16(z/L)\}^{-1/4}; \quad z/L < 0 \tag{2}$$

$$\phi_m(z/L) = 1 + 5(z/L); \quad z/L > 0. \tag{3}$$

An alternative formulation for the stable case, proposed by Beljaars and Holtslag (1991), is

$$\phi_m(z/L) = 1 + \frac{z}{L}\left\{a + b\, e^{-d\frac{z}{L}}\left(1 + c - d\frac{z}{L}\right)\right\} \tag{4}$$

where $a = 1$, $b = 0.667$, $c = 5$, and $d = 0.35$.

In local similarity theory, the turbulent fluxes and stability are not constrained to be constant with height and the non-dimensional shear takes the form (e.g. Wyngaard 1973; Nieuwstadt 1984; Sorbjan 1986)

$$\phi_{ml}(z/\Lambda) = \frac{\kappa z}{u_{*l}}\frac{\partial u}{\partial z} \tag{5}$$

where the subscript l refers to the local value at a given height, and Λ is the value of L calculated from the local height-dependent fluxes. This theory recognizes that local fluxes should be related to the local shear and stability. When the height-dependence of the fluxes of momentum and buoyancy can be neglected, local similarity reduces to MO similarity. In this sense, MO similarity is a subset of local similarity. Studies that report ϕ_m based on measuring fluxes at a single level, e.g. the 10 m level on a tower, are formally evaluating local similarity theory (ϕ_{ml}) due to a lack of information on the change in the fluxes with height. The distinction between MO and local similarity theory becomes uncertain in studies that do not evaluate the height-dependence of the flux. Previous single-level studies have been postulated as MO similarity by implicitly assuming that the height-dependence of the flux can be neglected. This is probably a good assumption in the lowest few tens of metres in the daytime convective boundary layer. However, with internal boundary layers or morning and evening boundary layer transition periods, which are the main source of near-neutral data in many field programmes, this assumption breaks down. Therefore, some observational studies have computed stability functions intended for MO similarity when in actuality the stability functions are more appropriate to local similarity theory.

According to traditional similarity theory, the non-dimensional shear does not depend on any characteristics of the surface. Historically, the surface has been represented by the roughness length (z_o), which is the constant of integration obtained when integrating Eq. (1) with respect to z to obtain $\psi_m(z/L)$ (e.g. Paulson 1970). Over solid surfaces, the roughness length is usually considered to be a constant for a given location, and dependent on wind direction over heterogeneous surfaces. The roughness length for momentum is found to be directly related to the physical size and spacing of the roughness elements of the surface.

Unlike conditions over land, the sea surface roughness field consists of a broad band of waves which are generated by and interact with the mean wind. With accelerating winds, surface gravity waves grow by extracting momentum from the mean flow, while with decelerating winds and mature waves, the surface wave field extracts considerably less energy or even loses energy to the mean flow. The wind and waves in the coastal zone are often in non-equilibrium due to bathometry and limited fetch. Sea surface roughness lengths are much smaller than typical land values. Over the sea, the roughness length has been parametrized using the Charnock (1955) relationship, which predicts that the roughness length is proportional to the wind stress.

Numerous studies have found that for a given wind speed and stability parameter (z/L), the drag coefficient and roughness length are larger over young and developing wave fields compared with older wave fields that are more in quasi-equilibrium with the wind (e.g. Kitaigorodskii 1970; Snyder et al. 1981; Geernaert et al. 1987; Donelan, 1990; Smith et al. 1992; Donelan et al. 1993; Vickers and Mahrt 1997a). Wave age is often used as a measure of the maturity of the wave field, and is typically calculated as the ratio of the wave phase speed of the dominant wave mode (C_p) (assuming a dominant mode is well defined) to either the friction velocity or the wind speed at some level near the surface (e.g. 10 m). The effect of wave age has been parametrized within the existing framework of similarity theory by formulating the roughness length, or equivalently the neutral drag coefficient, as a function of wave age (e.g. Toba and Koga 1986; Maat et al. 1991; Donelan 1990; Smith et al. 1992).

Some studies have approached the influence of wave state by directly examining the dependence of ϕ_m (or equivalently ψ_m and a specified z_o) on wave state rather than adjusting the roughness length. Bergström and Smedman (1995) found that the non-dimensional shear was less with young waves (small wave-age parameter) compared to old waves, but concluded that the relationship was not statistically significant, perhaps due to their small range of conditions. However, their result is consistent with enhanced mixing and stress over young, growing waves. Davidson (1974) found that isolating the dependence of the non-dimensional shear on wave state is sensitive to how the stability dependence is removed. He concluded that for his open-ocean dataset, the non-dimensional shear increased with wave age, in contrast to traditional MO similarity theory which contains no wave state dependence. In his dataset, the wave field was characterized as surge swell (values of $C_p/u_* > 25$) representative of an older decaying wave field, conditions were always stable ($z/L > 0$), and almost all results were based on a single vertical level (8 m). Consistent with enhanced mixing over younger waves, Davidson (1974) suggested a form $\psi_m(z/L, C_p/u_*)$, where ψ_m decreased with wave age for $C_p/u_* > 25$.

Miller et al. (1997) reported observational evidence in near-neutral conditions for an intermediate layer of order 10 m thickness located above the wave boundary layer (order 1 m) and below an outer logarithmic layer. In the intermediate layer, the wind shear was substantially less than predicted by MO similarity (smaller ϕ_m than predicted). They found that the wave-induced stress associated with atmospheric motions in phase with

the surface waves was significant in the underlying wave boundary layer and was small in the intermediate layer.

In the coastal waters of the Baltic Sea, Smedman et al. (1995) found that in stable flow, the non-dimensional wind shear and temperature gradient based on observations 8 m above the sea surface did not always agree with traditional MO similarity. They attributed this to an extremely shallow surface layer due to the presence of a low-level jet (30 to 150 m) and suggested that the height of the jet may be an important length scale. Smedman et al. (1995) proposed that the low-level jet suppresses low-frequency motions thus reducing the transport and increasing the non-dimensional wind shear. They found general agreement with traditional MO similarity at the same site during similar stability when no low-level jet was detected.

Grant (1992) suggests that the non-dimensional gradient $\phi(z/L)$ for the near-neutral boundary layer should be generalized to be of the form $\phi(z/h, h/L, u_*/fh)$ in order to include the influence of boundary layer depth (h) on the non-dimensional shear. Khanna and Brasseur (1997) consider the form $\phi(z/L, h/L)$ where their ϕ is the non-dimensional gradient of an arbitrary variable. In the large eddy simulation results of Khanna and Brasseur (1997), the non-dimensional shear decreases above the surface layer; this is also observed by Smedman and Johansson (1997) in shallow off-shore boundary layers. Apparently, the vertical gradient decreases more rapidly with height above the surface than does the flux. No specific formulation for a generalization of ϕ to include the dependence on boundary layer depth has been attempted. If the influence of boundary layer depth on ϕ_m extends downward to the surface, or if the influence of wave state on ϕ_m extends upward above the wave boundary layer, then both local and MO similarity theory break down. We intend to consider several possibilities: (a) MO similarity with existing stability functions is valid; (b) MO similarity theory is valid but the traditional stability functions require modification; (c) MO similarity is not valid but local similarity is appropriate with possible modification of the stability functions; and (d) both local and MO similarity theory are invalid and additional information such as boundary layer depth and wave state are required.

3. DATASET

The full RASEX instrumentation is described in Barthelmie et al. (1994) and Højstrup et al. (1997). Data used in this study were collected at the sea mast west tower located 2 km off the coast of Lolland, Denmark in 4 m of water. Observations taken from April through November 1994, including the intensive campaigns during the spring and autumn, are considered. The off-shore tower site is representative of an inland sea or large lake, with only small amplitude swell and predominantly wind driven waves with characteristic amplitudes less than 1 m and wavelengths less than 16 m (Vickers and Mahrt 1997a). In strong on-shore flow, the wave boundary layer may sometimes include the lowest turbulent flux measurement level at 3 m (Hare et al. 1997). The lowest observational level used in this study (6 m) is expected always to be above the top of the wave boundary layer based on the maximum observed wavelength. Shallow IBLs are common in off-shore flow where the fetch ranges from 2 to 5 km (Mahrt et al. 1998). On-shore flow, where the fetch ranges from 15 to 25 km, is still fetch-limited compared to the open ocean.

Fast-response (20 Hz) observations from Gill/Solent sonic anemometers (hereafter sonics) positioned 6, 10, 18 and 32 m above the sea surface were used to estimate the turbulent wind stress and buoyancy flux profiles. Turbulence measurements from

the instrument at the 3 m level were excluded in this study due to potential flow-distortion problems. Fluxes calculated from the 45 m level sonic data were found to be erratic and unreliable, presumably due to an instrumental problem, and were excluded. The tilt-correction method used for the sonics was presented in Mahrt *et al.* (1996). The buoyancy flux was calculated from the sonic virtual-temperature fluctuations, after applying a correction for acoustic wave bending that can be important in strong winds. Vertical profiles of wind speed were measured using cup anemometers (P224b sensor) located 7, 15, 20, 29 and 38 m above the sea surface. Time periods where the cup anemometer wind speed was less than 2.5 m s^{-1} were excluded; because the cup anemometers were calibrated for the generally strong winds at the site, readings of less than 2.5 m s^{-1} are not reliable. Temperature profiles were measured using a thermometer at 10 m (Risø PT 100), and temperature-difference sensors (Risø PT 500) to provide the vertical gradient of temperature over the layers 10 to 24 m and 10 to 47 m. The fluctuating wave height was measured using an acoustic wave recorder. A characteristic wave amplitude, wave phase speed and wavelength were calculated as described in Vickers and Mahrt (1997a). All time periods with wind direction from the sector including 339 deg. through 106 deg. were excluded, because of potential tower interference and possible flow distortion due to wind turbines located north-east of the tower.

The sonic and cup anemometer and wave recorder measurements were subjected to quality control screening as described in Vickers and Mahrt (1997b). The automated quality control procedure identifies periods with potential problems with instruments or data recording. The package of tests checks for excessive electronic spiking, inadequate amplitude resolution, signal dropout, unrealistic magnitude, extreme higher moment statistics and near discontinuities in the first two moments. Visual inspection of all data flagged by the automated procedures was carried out, either to verify an instrument problem or to identify unusual but plausible atmospheric behaviour. In the former case, the flag was verified and the data were eliminated.

Direct observations of IBL depth at the site were not routinely available during RA-SEX. Profiles of potential temperature, humidity and winds, measured by tethersondes released from land in the vicinity of the site during 12 different days in October and early November 1994, were examined. A parametrized IBL depth (e.g. Højstrup, 1981)

$$h = C\sigma_w(X/u),\qquad(6)$$

where σ_w is the vertical velocity fluctuation, X is the fetch distance and C is an empirical coefficient, was found to correlate reasonably well with the IBL depth as inferred from the tethered balloon soundings for the limited number of comparisons available. We found that setting $C = 0.4$ gave a better fit to the data than the original coefficient of unity, and use $C = 0.4$ in all further calculations. Using the vertical velocity fluctuations from the 18 m sonic, the 38 m wind speed from the cup anemometer and the actual fetch distance, the parametrized h at the tower location varies from a minimum of 20 m in off-shore flow (1:100 stable IBL growth rate) to a maximum of 400 m in on-shore flow (1:30 unstable IBL growth rate). We note that u in Eq. (6) should represent the mean wind at the top of the IBL, which results in an iterative expression for h. Here, we approximate u at height h using the 38 m wind speed.

(a) Fluxes

Eddy correlation fluxes of momentum and virtual temperature were calculated from sonic anemometers at 4 levels (6, 10, 18 and 32 m) to estimate profiles of the wind

stress and Obukhov length. An averaging time-scale of 10 minutes was selected to define the turbulent fluctuations, and the flux computed from such fluctuations was averaged over one-hour periods. Therefore, the fluxes include all motions on time-scales of 10 minutes or less down to the smallest resolvable scales determined by the sampling rate (20 Hz). These averaging times were chosen to optimize the correlation between the mean wind speed and the wind stress (Mahrt *et al.* 1996). Averaging times longer than one hour incorporate too much non-stationarity, and shorter averaging times do not include enough samples. Elimination of records with large non-stationarity and flux sampling errors are discussed in the appendix. The wind stress was calculated as the vector magnitude of the one-hour averages of the stress components.

(b) Wind profiles

The wind shear was estimated by applying the method of least squares to fit a second-order polynomial in $\ln(z)$ to the profiles of one-hour mean wind speed from the cup anemometers at 5 levels (7, 15, 20, 29 and 38 m), and also a derived level at the roughness height (z_o) where the wind speed was assumed to be zero. The precise heights of the wind speed measurements were adjusted to account for the fluctuating mean sea level. The wind speeds from the cup anemometers were re-calibrated using the post-experiment calibration coefficients (Højstrup, personal communication). The wind shear was evaluated analytically at the flux measurement heights (6, 10, 18 and 32 m) using the coefficients of the second-order polynomial fit to the wind speed profile as in Högström (1988). The Charnock relationship with a coefficient of 0.017 (Garratt 1977) was used as a lower-boundary condition for the fit. The fit to the wind speed profile was not sensitive to the choice of this coefficient nor application of a wave-age dependent Charnock relationship.

As a sensitivity study, the wind speed profiles were fitted using the cup anemometer wind speeds alone, the sonic speeds alone and a combined set of cup and sonic wind speeds. We also calculated the shear using finite differences applied to adjacent cup levels, differencing with respect to both linear z and $\ln(z)$. In most instances, the profile of wind speed from the cups was smoother than both the profile from the sonics and the profile from the combined cup and sonic set. In terms of variance explained, the cup wind speed profiles were better represented by the second-order polynomial than were the profiles from the sonic speed measurements or the combined cup and sonic set. The root-mean-square error of the model fit to the wind speed profile evaluated at the 5 cup anemometer levels ranged from 0.03 m s^{-1} to 0.19 m s^{-1} and averaged 0.09 m s^{-1}.

4. NON-DIMENSIONAL SHEAR

The observed dependence of ϕ_{ml} on z/Λ for all the data including all 4 vertical levels and both on-shore and off-shore flow regimes is shown in Fig. 1. The observed ϕ_{ml} is less than the traditional prediction (Eqs. (2)–(4)) for the entire range of stability (greater stress relative to the shear). The near-neutral $(-0.01 < z/\Lambda < 0.01)$ value of ϕ_{ml} is 0.95 with $\kappa = 0.40$. The standard error of the average ϕ_{ml} for z/Λ categories is relatively small for the near-neutral categories, and larger for unstable and stable categories where the number of observations is less.

For estimating ϕ_m for MO similarity at the 10 m level, we excluded cases with the largest vertical flux divergence based on the fluxes at the 6, 10 and 18 m levels. This flux divergence criterion excluded approximately one-half of the data. For the remaining cases used in calculating ϕ_m, the magnitude of the stress divergence for the layer from
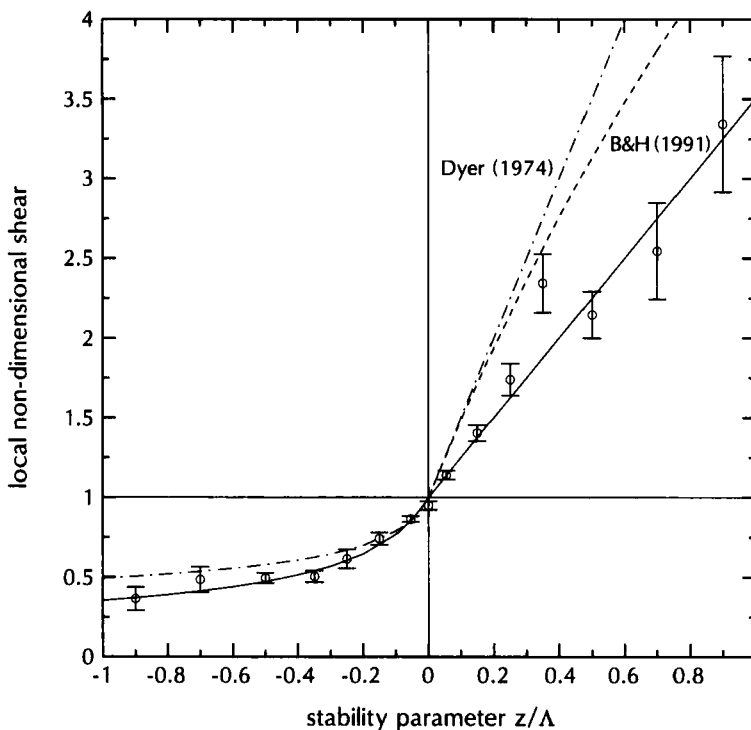
Figure 1. The mean (circles) and plus and minus one standard error of the local non-dimensional shear (ϕ_{ml}) for stability (z/Λ) categories (see text) for all the data. The solid curve is a fit to the data: $\phi_{ml} = \{1 - 7(z/\Lambda)\}^{-1/2}$; $z/\Lambda < 0$, and $\phi_{ml} = 1 + 2.5(z/\Lambda)$; $z/\Lambda > 0$, where Λ is the Obukhov length based on local fluxes. The dash-dot curve is the traditional Dyer (1974) parametrization. The dashed curve is the Beljaars and Holtslag (1991) formula.

6 m to 18 m was always less than 8×10^{-3} m s^{-2} and averaged 5×10^{-4} m s^{-2}. As we found for local similarity, the non-dimensional shear of MO similarity theory (ϕ_m) is also less than the traditional prediction (Fig. 2). The mean ϕ_m at 10 m for weakly stable conditions is larger than ϕ_{ml}, closer to both the predictions (Eqs. (3)–(4)) and similar to the estimate of ϕ_{ml} when excluding off-shore flow cases (Fig. 3). This reflects the fact that large flux divergence is common in off-shore stable flow. In this regard, eliminating periods with large flux divergence is similar to eliminating periods with stable off-shore flow. In unstable conditions, the observed 10 m ϕ_m is less than ϕ_{ml}, further from the prediction (Eq. (2)) and similar to ϕ_{ml} when excluding shallow IBL cases (Fig. 4). For the unstable case, eliminating periods with large flux divergence also tends to eliminate periods with shallow IBL depth. We conclude that eliminating convective cases with large flux divergence does not improve the agreement between the observed ϕ_m and the traditional prediction (Eq. (2)).

Note that the range of the stability parameter for the ϕ_m dataset, where $z = 10$ m, is considerably less than for the ϕ_{ml} dataset which includes $z = 6$, 10, 18 and 32 m. The standard error bars are larger for ϕ_m than for ϕ_{ml} partly due to the smaller sample size.

The mean $\phi_{ml}(z/\Lambda)$ partitioned into on-shore and off-shore flow categories is shown in Fig. 3. In this dataset, the majority of the strongly convective cases are found in on-shore flow while the majority of the strongly stable cases are found in off-shore flow. This complicates attempts to isolate the effects of stability and fetch. The range of z/Λ for an individual stability category was expanded in Fig. 3 compared to Fig. 1,
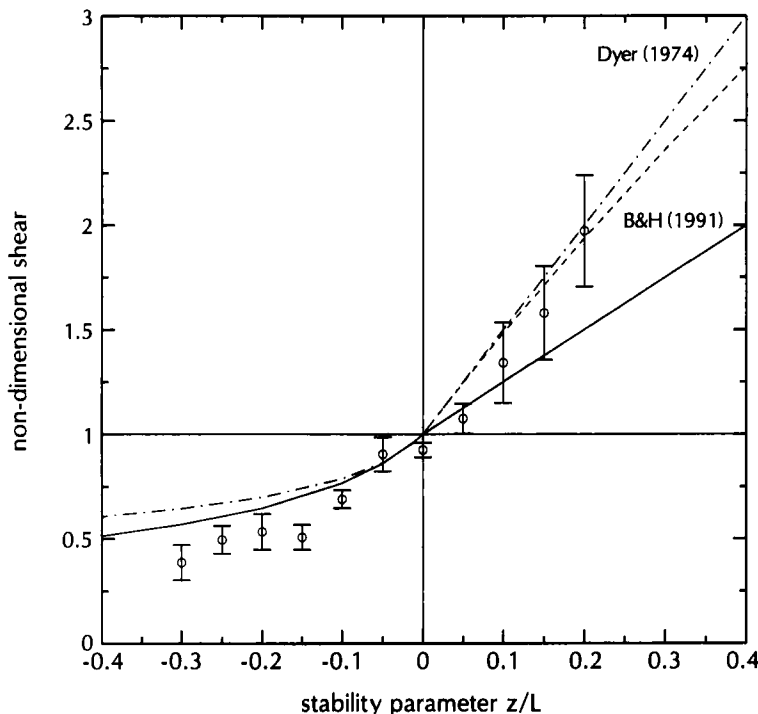
Figure 2. The mean and standard error of the non-dimensional shear (ϕ_m) for 10 m data only for stability (z/L) categories (see text). The solid curve is a fit to the local non-dimensional shear ϕ_{ml} (as in Fig. 1). The dash-dot curve is the traditional Dyer (1974) parametrization. The dashed curve is the Beljaars and Holtslag (1991) formula.

to ensure an adequate number of samples in each stability category when partitioning the data by both stability and flow regime. For off-shore neutral and stable flow, ϕ_{ml} is significantly less than predicted by previous relationships. In the transition region downstream from a rough-to-smooth roughness change, the mean shear may adjust more rapidly to the smoother ocean surface compared to the stress, preventing equilibrium between the stress and the shear (Peterson 1969). As a result, the non-dimensional shear may be smaller in the coastal zone than that predicted by traditional similarity theory. A mechanism to account for the difference between the on-shore and off-shore flow unstable cases is discussed next.

(a)   IBL depth

The stability dependence of ϕ_{ml} for two z/h categories is shown in Fig. 4 where h is the IBL depth estimated from Eq. (6). The largest values of z/h (small h) occur in off-shore flow due to the shorter fetch, and partitioning the data by z/h also tends to partition the data into off-shore and on-shore flow regimes. Therefore, other factors in addition to IBL depth may cause differences between the two z/h classes.

In convective IBLs, ϕ_{ml} increases with increasing z/h with the exception of the most unstable category, that also has the least amount of data. We attribute the increase of ϕ_{ml} with increasing z/h to suppression of the largest convective eddies by the shallow IBL top (Mahrt *et al.* 1998), which acts to reduce the stress relative to the shear. Multi-resolution spectra (Howell and Mahrt 1997) of the wind stress from the 6 and 32 m levels support this theory in that lower-frequency (large eddy) transport is indeed suppressed
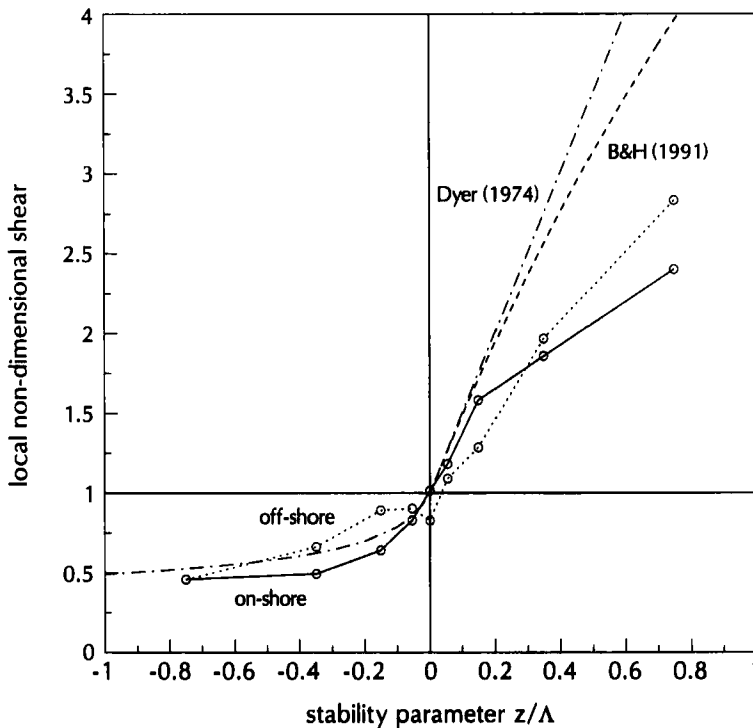
Figure 3.   The mean local non-dimensional shear (ϕ_{ml}) for stability (z/Λ) categories (see text) for on-shore flow (solid) and off-shore flow (dotted). The dash-dot curve is the traditional Dyer (1974) parametrization. The dashed curve is the Beljaars and Holtslag (1991) formula.

by shallow IBL depth (Fig. 5). The multi-resolution spectra orthogonally decompose the flow into simple unweighted averages for different averaging windows. These spectra yield results similar to Fourier spectra but satisfy Reynolds averaging at all scales and do not assume periodicity.

In contrast to unstable conditions, the spectra for neutral and stable conditions show little difference in the scale-dependence of the stress over a wide range of z/h. Our hypothesis is that in neutral and stable conditions, the eddies are too small to be suppressed by the shallow IBL depth.

The agreement with traditional similarity for convective IBL cases is better when combining on-shore and off-shore flow (Fig. 1), than when partitioning the data by either flow regime or z/h (Figs. 3 and 4). This agreement is somewhat circumstantial. In on-shore flow, where the IBL depth is typically large compared to the observation height, and where we would expect the best agreement with the traditional parametrization, ϕ_{ml} is less than predicted. In off-shore flow with shallow convective IBLs, ϕ_{ml} is larger than predicted. *These data suggest that for the convective case, ϕ_{ml} is less than predicted by traditional similarity but increases with increasing z/h.*

In stably stratified IBLs, ϕ_{ml} decreases with increasing z/h (Fig. 4). That is, shallow stable IBLs lead to relatively large stress and therefore smaller ϕ_{ml} than predicted. We attribute this to the top-down nature of the turbulence in the presence of shallow stable IBLs in advective conditions where the stress decreases with height more slowly than the mean shear, or where it may even increase with height (Fig. 6). This is apparently due to suppression of turbulence near the surface by the stratification in concert with
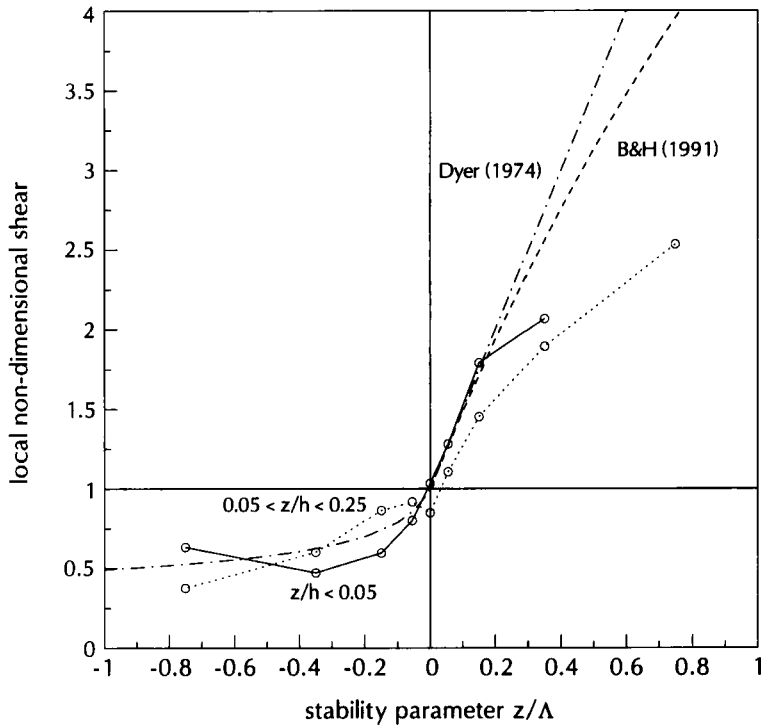
Figure 4. The mean local non-dimensional shear (ϕ_{ml}) for stability (z/Λ) categories (see text) for two internal boundary layer (IBL) depth (z/h) categories: (i) $z/h < 0.05$ (solid); and (ii) $0.05 < z/h < 0.25$ (dotted), where h is the parametrized IBL. The dash-dot curve is the traditional Dyer (1974) parametrization. The dashed curve is the Beljaars and Holtslag (1991) formula.

shear-generation of turbulence aloft, although horizontal advection of turbulence may also be important. The composited wind profiles for this case (not shown) correspond to increasing mean shear with height. The elevated shear may be associated with flow acceleration resulting from partial decoupling from the sea surface, sometimes observed with the flow of warmer air over cooler water (Smedman *et al.* 1995). When the stress increases with height the usual atmospheric boundary layer is turned upside down, in that the primary source of the turbulence is aloft rather than at the surface. The physical interpretation of the IBL depth is ambiguous in such cases.

Temperature advection is also important in off-shore flow. Non-zero heat flux is forced primarily by temperature advection. That is, the heat flux divergence is balanced by temperature advection since the local time-change of temperature is usually small. Since z/L depends on the heat flux, z/L is correlated with temperature advection. Therefore, any stability-dependent non-dimensional quantities over the sea automatically contain advective effects, particularly in the coastal zone.

(b) Wave age

The stability dependence of ϕ_{ml} for two wave age (C_p/u_*) regimes is shown in Fig. 7. Young, growing-wave fields preferentially occur with off-shore flow, but are also commonly found in strong on-shore flow. In stable conditions, ϕ_{ml} increases significantly with increasing wave age as also observed by Bergström and Smedman (1995) and Davidson (1974). The self-correlation between wave age and ϕ_{ml} (both
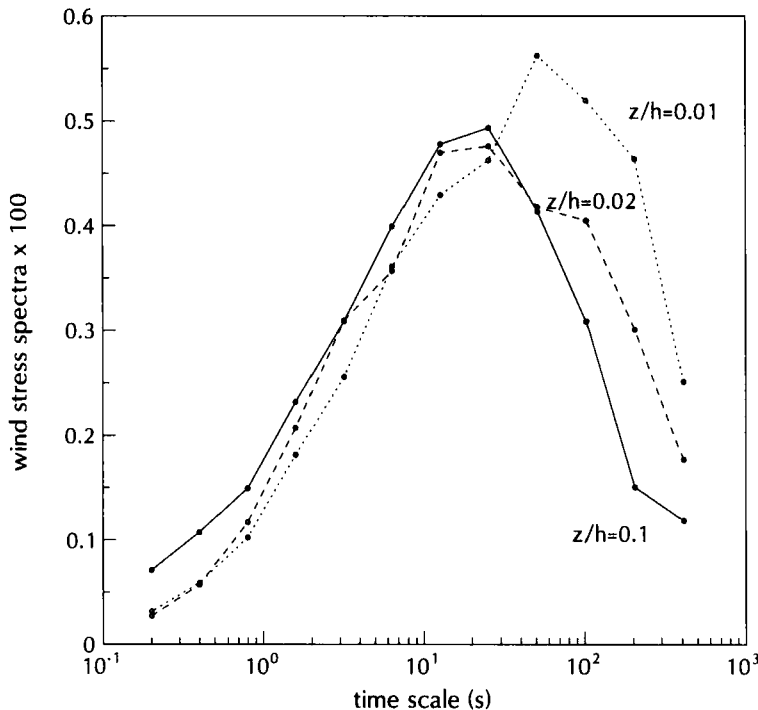
Figure 5.   Average multi-resolution spectra of the one-hour average kinematic wind stress (m^2 s^2 × 100) at the 6 m level in unstable conditions for three z/h categories (see text): (i) $z/h = 0.1$ (solid); (ii) $z/h = 0.02$ (dashed); and (iii) $z/h = 0.01$ (dotted) where h is the parametrized internal boundary layer depth. The time-scale axis is analogous to the period in Fourier analysis.

contain u_*) may influence the result. The self-correlation between z/L and ϕ_m can also be large (L contains u_*^3). We have attempted to reduce the self-correlation by jointly stratifying ϕ_{ml} by both z/Λ and C_p/u_* in Fig. 7. In a separate calculation, we partitioned the data into C_p/u_t wave-age regimes, where this wave-age parameter is based on u_t, the estimated wind speed at the top of the wave boundary layer, instead of u_*, and thus is not subject to self-correlation. This calculation confirmed a real dependence of ϕ_{ml} on wave state. We conclude *that in stable conditions, the mean shear does not completely adjust to the growing-wave field leading to a dependence of ϕ_{ml} on wave age.*

The possible dependence of ϕ_{ml} on wave age contradicts the assumption of similarity theory that the local flux-gradient relationship in the surface layer is independent of surface conditions. In traditional similarity theory for the surface layer (above the wave boundary layer), the influence of surface characteristics is included in the roughness length which appears in the vertical integration of ϕ_{ml} downward to the surface. In this dataset, the observation heights are well above the estimated wave boundary layer height, so that dependence of ϕ_{ml} on wave state is not expected on the basis of traditional similarity theory.

For unstable conditions, ϕ_{ml} is observed to be larger over younger waves, contrary to the result found for stable flow (Fig. 7). This may be due to the dominant influence of shallow IBL depth rather than wave state in modifying ϕ_{ml} for convective cases (section 4(a)). It may also be related to correlation between wave age and other processes related to flow direction, since the difference between ϕ_{ml} for younger waves compared
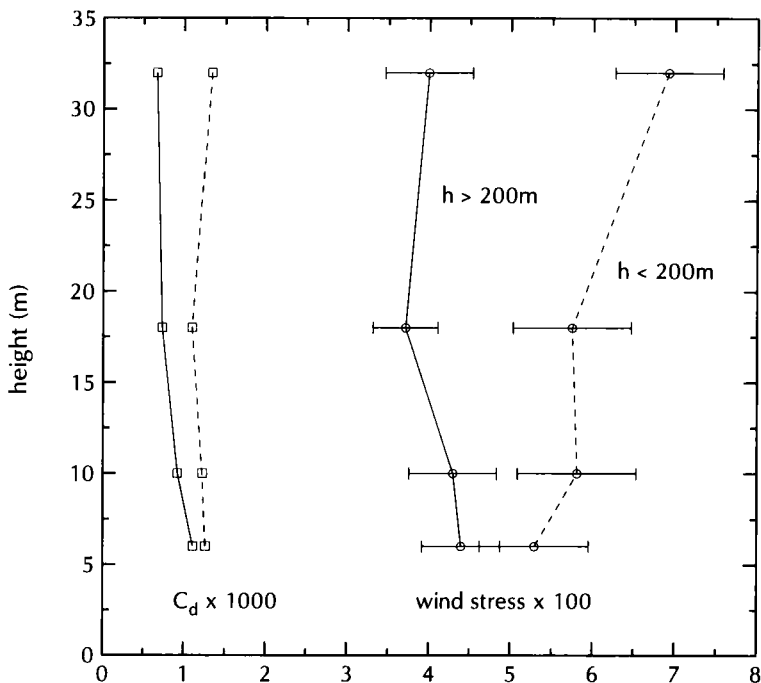
Figure 6. Average profiles of the kinematic wind stress (m²s² × 100) and drag coefficient (C_d × 1000) in stable stratification ($0.05 < z/L < 0.3$) for $h > 200$ m (solid) and $h < 200$ m (dashed) where h is the parametrized internal boundary layer depth, and Obukhov length L is calculated using the average fluxes from the 6 and 10 m levels. The average stability (z/L) and wind speed profile for both h categories are nearly identical.

with older waves is similar to the difference when partitioning the data by flow direction (Fig. 3).

5. NEW FORMULATION

With off-shore flow in the coastal zone, shallow IBL's are common due to short fetch. Significant vertical stress and buoyancy flux divergences are typical due to shallow IBL depth and strong temperature advection. The wind and waves can be in non-equilibrium due to the bathometry and limited fetch. Relatively large stress generated over land may be advected over the water. The mean flow normally accelerates due to smaller surface roughness over the water. All of these mechanisms influence the non-dimensional shear.

We expect that the conditions required for application of similarity theory will be best satisfied when advective effects are minimal (on-shore flow) and the observation height is sufficiently below the IBL depth ($z/h < 1/4$). The stability dependence for data satisfying these conditions is shown in Fig. 8 and a fit to the data is:

$$\phi_{ml} = \{1 - 35(z/\Lambda)\}^{-1/4}; \; z/\Lambda < 0 \tag{7}$$

$$\phi_{ml} = \{1 + 16(z/\Lambda)\}^{1/3}; \; z/\Lambda > 0. \tag{8}$$

For this reduced dataset, a von Karman constant (κ) equal to 0.39 is required to make $\phi_{ml}(z/\Lambda = 0)$ equal to unity, and the coefficients in Eqs. (7)–(8) are based on $\kappa = 0.39$. The model predicts unstable values of ϕ_{ml} that are approximately 15–20% smaller
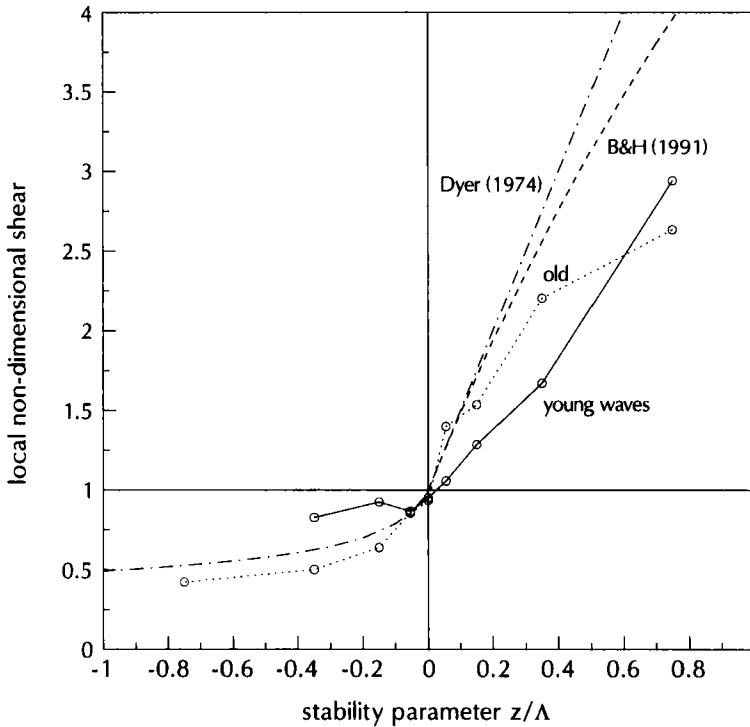
Figure 7. The mean local non-dimensional shear (ϕ_{ml}) for stability (z/Λ) categories (see text) for two wave-age (C_p/u_*) categories: (i) $C_p/u_* < 15$ (solid); and (ii) $C_p/u_* > 15$ (dotted), where C_p is the phase speed of the dominant wave mode. The dash-dot curve is the traditional Dyer (1974) parametrization. The dashed curve is the Beljaars and Holtslag (1991) formula.

than the Dyer (1974) formula (greater stress relative to the shear). It is not clear if the relatively weak shear observed here is related to the weak shear layer observed by Miller *et al.* (1997). For stable conditions, Eq. (8) predicts values of ϕ_{ml} significantly less than Dyer (1974) for values of z/Λ exceeding 0.2. The deviation of the non-dimensional shear from Dyer's formula is in the same direction as the Beljaars and Holtslag (1991) correction, but much greater in magnitude. Howell and Sun (1999) further document the overprediction of ϕ_m by traditional stability functions for strong stability, although the deviations from Dyer are greater in the present study.

To better isolate the potential influence of IBL depth and wave age on ϕ_{ml}, we calculated the residuals from the model, defined as the observed ϕ_{ml} minus Eqs. (7)–(8), and partitioned them by z/h and wave-age categories for unstable and stable periods. The observed ϕ_{ml} dataset includes all the on-shore and off-shore flow periods.

For unstable conditions, the ϕ_{ml} residuals increase with increasing z/h for $z/h < 1/3$ for all wave-age regimes except the youngest wave-age category (Table 1). The main effect here appears to be due to suppression of large convective eddies by shallow IBL depth (section 4(a)). For very shallow IBL depth ($z/h > 1/3$), ϕ_{ml} decreases with z/h. We attribute this to the elevated generation of turbulence. In unstable flow, there is no clear relationship between the ϕ_{ml} residuals and wave age.

The dependence of the unstable ϕ_{ml} residuals on z/h suggests including the dependence of the non-dimensional shear on z/h for convective IBLs. Here we choose the
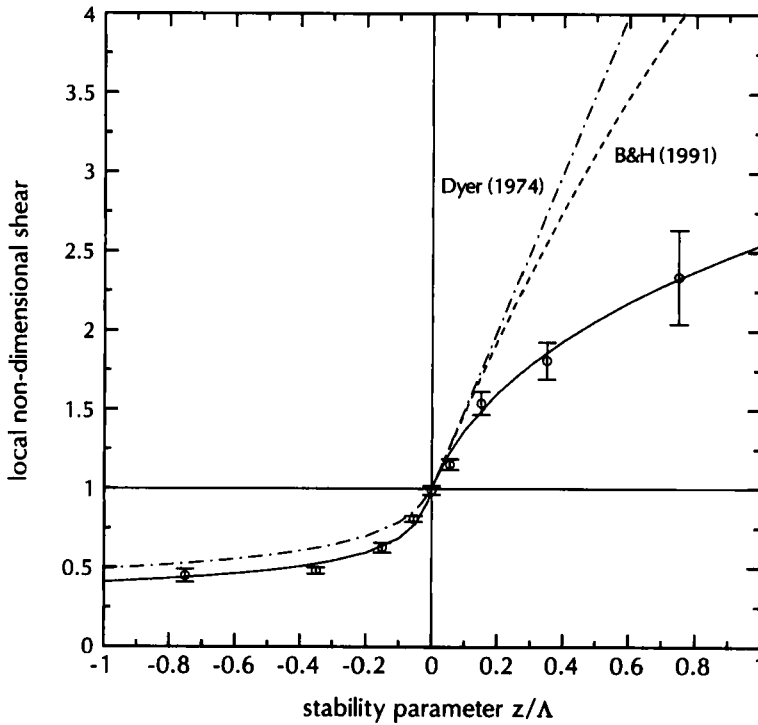
Figure 8.   The mean and standard error of the local non-dimensional shear (ϕ_{ml}) for stability (z/Λ) categories (see text) for conditions where similarity theory is expected to be most applicable: (i) minimal advective effects (on-shore flow only); and (ii) relatively deep boundary layer depth ($z/h < 1/4$). The solid curve is a fit to the mean values given by Eqs. (7)–(8) with von Karman constant $\kappa = 0.39$. The dash-dot curve is the traditional Dyer (1974) parametrization. The dashed curve is the Beljaars and Holtslag (1991) formula.

TABLE 1.   NON-DIMENSIONAL WIND SHEAR RESIDUALS (OBSERVED MINUS MODEL) FOR $z/\Lambda < 0$. THE COLUMNS ARE WAVE-AGE (C_P/u_*) CATEGORIES AND THE ROWS ARE z/h CATEGORIES. NUMBERS OF OBSERVATIONS ARE SHOWN IN PARENTHESIS

	5–10	10–15	15–20	20–25	25–30
0.32–1	−0.08 (20)	0.21 (13)	−0.06 (14)	−0.10 (09)	
0.1–0.32	0.01 (41)	0.30 (40)	0.00 (43)	−0.03 (17)	0.19 (04)
0.032–0.1	0.15 (08)	0.03 (39)	−0.02 (63)	0.01 (17)	−0.05 (06)
0.01–0.032	0.14 (07)	−0.03 (29)	−0.07 (34)	−0.09 (10)	

TABLE 2.   AS TABLE 1 BUT FOR $z/\Lambda > 0$

	5–10	10–15	15–20	20–25	25–30
0.316–1	−0.56 (43)	−0.29 (43)	−0.17 (26)	0.23 (08)	0.80 (10)
0.1–0.316	−0.11 (39)	−0.06 (62)	−0.03 (30)	0.07 (18)	1.42 (06)
0.0316–0.1	−0.03 (28)	−0.02 (52)	0.13 (21)	0.22 (21)	0.47 (05)
0.01–0.0316	−0.08 (16)	0.17 (19)	0.37 (10)	0.25 (10)	0.44 (03)

form for the unstable case as

$$\phi_{ml} = \{1 - 35(z/\Lambda)\}^{-1/4} + (-z/\Lambda)^{1/2}(z/h)(1 - 1.5z/h). \tag{9}$$

The term $(z/h)(1 - 1.5z/h)$ augments ϕ_{ml} from the stability-dependence prediction for the parameter range $0 < z/h < 2/3$, and reduces ϕ_{ml} for $z/h > 2/3$. We include this expression mainly to clarify the observed z/h dependence of ϕ_{ml} in convective IBLs. A more precise calibration of this expression would require a larger dataset and more explicit determination of the boundary layer depth.

For stable conditions, the ϕ_{ml} residuals clearly increase with increasing wave age for the entire range of z/h (Table 2). Theoretically, the shear in the surface layer should adjust to the stress such that ϕ_{ml} is independent of wave age. Apparently with stable stratification, the adjustment time-scale of the weak turbulence may be too slow to maintain equilibrium with the changing surface state. Consequently, the assumptions required for similarity theory are not met. As a possible result, the flux-gradient relationship (ϕ_{ml}) at the observational level now depends on wave state. A simple model which demonstrates the observed dependence of the ϕ_{ml} residuals on wave age for the stable case is

$$\phi_{ml} = \{1 + 16(z/\Lambda)\}^{1/3} + (z/\Lambda)^2(C_p/u_* - 18)/20, \tag{10}$$

where the coefficients (18 and 20) were determined using the average residuals for the wave-age categories in Table 2. The wave-age term augments the stability-dependent prediction of ϕ_{ml} for older-wave fields $(C_p/u_* > 18)$ and reduces ϕ_{ml} over younger waves. This model predicts zero wave-age influence for wave age equal to 18, which is smaller than the value of 25 thought to represent minimal wind–wave coupling (Volkov 1970).

In stable flow over young waves $(C_p/u_* < 20)$, the ϕ_{ml} residuals clearly become more negative with increasing z/h (stronger stress relative to the shear), while over older waves the dependence on z/h is weak (Table 2). The decrease in ϕ_{ml} with increasing z/h in stable flow was noted in section 4(a), and attributed to a possible top-down nature of the turbulent transport. Table 2 shows that the combined influence of young waves and shallow stable IBL depths leads to the largest negative ϕ_{ml} residuals (smallest non-dimensional shear compared to Eqs. (7)–(8)) in this dataset. In this situation, the stress is large relative to the shear due to the influence of wind–wave coupling and the elevated generation of turbulence.

6. CONCLUSIONS

For convective internal boundary layers in the coastal zone, the non-dimensional wind shear is less than predicted by traditional similarity but increases with increasing z/h. The largest convective turbulent eddies are suppressed by the top of the internal boundary layer, leading to an increase in the non-dimensional shear with increasing z/h.

In stable internal boundary layers, elevated generation of turbulence can lead to an upside down boundary layer where the stress may even increase with height. As a result, the non-dimensional shear decreases with increasing z/h. This is apparently due to suppression of turbulence near the surface by the stratification and shear-generation of turbulence aloft. However, advection of stress may also be important.

In stable stratification, smaller non-dimensional shear is observed over young growing waves compared to older waves. We speculate that with the long adjustment time-scale and weaker turbulence associated with stable stratification, the mean shear in the

coastal zone does not completely adjust to the wind–wave coupling influence on the stress. In addition, the surface waves may effectively perturb the adjacent stable atmosphere, since vertical velocity fluctuations in a stratified atmosphere induce temperature-related pressure perturbations (such as internal gravity waves). Therefore, the non-dimensional shear depends on wave state, even though the observational levels are well above the wave boundary layer where individual eddies are coherent with surface waves. For convective and neutral conditions, wave state does not appear to have an influence on the non-dimensional shear.

A formulation for the non-dimensional shear (Eqs. (7)–(8)) in the marine surface layer is constructed as a function of the traditional stability parameter, based on data where the conditions required for application of similarity theory are expected to be met. Compared to the traditional land-based parametrization, the new formulation predicts slightly smaller non-dimensional shear for unstable conditions and significantly smaller non-dimensional shear for strong stability. The formulation is generalized to include the influence of internal boundary layer depth (Eq. (9)) and wave state (Eq. (10)). This formulation requires evaluation from a more extensive dataset to better isolate the influences of stability, internal boundary layer depth and wave state, that are sometimes inter-correlated. The formulation of the non-dimensional shear has been posed in terms of local scaling instead of Monin–Obukhov similarity theory. However, the distinction in the literature is not always clear, since the vertical flux divergence is usually not available and the difference between the flux at the observational level and the surface is not known.

APPENDIX

Elimination of records

The flux sampling errors and non-stationarity for momentum and buoyancy were evaluated following Vickers and Mahrt (1997b) and Mahrt (1998). All vertical levels of data for each one-hour time period with flux sampling errors exceeding prescribed thresholds for any of the 4 levels for either the momentum or the buoyancy flux were eliminated from further analysis. Using the notation in Vickers and Mahrt (1997b), the thresholds used were: (i) 6 for extreme subrecord flux outliers (event); (ii) 1 for the relative systematic flux error (RSE) associated with the flux on scales larger than the 10-minute average; (iii) 0.75 for the relative random flux error due to inadequate sample size (RFE); and (iv) 5 for non-stationarity of the flux (NR, defined in Mahrt 1998; his Eq. (11)). The averaging time-scale used in the flux sampling error analysis was: (i) 5-minutes for event and RFE, resulting in 12 independent estimates of the flux in each one-hour time period; (ii) 5- and 10-minute fluxes for estimation of the scale-dependence of the flux (RSE); and (iii) 100-second fluxes for the non-stationarity ratio NR. All the flux sampling criteria applied to the fluxes of momentum and buoyancy for all 4 vertical levels combined removed 35% of the one-hour time periods. Excluding data based on the flux sampling criteria reduced the scatter in the composited profiles of the wind stress and buoyancy flux. After the flux sampling screening, the final flux dataset consisted of

415 observations in off-shore flow and 483 observations in on-shore flow. No attempt was made to correct for potential flow distortion, which may contribute to scatter in the relationships.

REFERENCES

Barthelmie, R. J., Courtney, M. S., Højstrup, J. and Sanderhoff, P.   1994   'The Vindeby Project: A Description'. Report R-741(EN), Risø National Laboratory, DK4000, Roskilde, Denmark

Belcher, S. E. and Hunt, J. C. R.   1998   Turbulent flow over hills and waves. *Ann. Rev. Fluid Mech.*, **30**, 507–538

Beljaars, A. C. M. and Holtslag, A. A. M.   1991   Flux parametrization over land surfaces for atmospheric models. *J. Appl. Meteorol.*, **30**, 327–341

Bergström, H. and Smedman, A.   1995   Stably stratified flow in a marine atmospheric surface layer. *Boundary-Layer Meteorol.*, **72**, 239–265

Businger, J. A., Wyngaard, J. C., Izumi, Y. and Bradley, E. F.   1971   Flux profile relationships in the atmospheric surface layer. *J. Atmos. Sci.*, **28**, 181–189

Chalikov, D. V. and Belevich, M. Y.   1993   One-dimensional theory of the wave boundary layer. *Boundary-Layer Meteorol.*, **63**, 65–96

Chalikov, D. V. and Makin, V. K.   1991   Models of the wave boundary layer. *Boundary-Layer Meteorol.*, **56**, 83–99

Charnock, H.   1955   Wind stress over a water surface. *Q. J. R. Meteorol. Soc.*, **81**, 639–640

Davidson, K. L.   1974   Observational results on the influence of stability and wind–wave coupling on momentum transfer and turbulent fluctuations over ocean waves. *Boundary-Layer Meteorol.*, **6**, 305–331

Donelan, M. A.   1990   Air–sea interaction. Pp. 239–292 in *Ocean Engineering Science* Eds. B. LeMehaute and D. M. Hanes. John Wiley and Sons, New York, USA

Donelan, M. A., Dobson, F. W., Smith, S. D. and Anderson, R. J.   1993   On the dependence of sea surface roughness on wave development. *J. Phys. Oceanogr.*, **23**, 2143–2149

Dyer, A. J.   1974   A review of flux-profile relationships. *Boundary-Layer Meteorol.*, **7**, 363–372

Garratt, J. R.   1977   Review of drag coefficients over oceans and continents. *Mon. Weather Rev.*, **105**, 915–929

   1990   The internal boundary layer—a review. *Boundary-Layer Meteorol.*, **50**, 171–203

Geernaert, G. L., Larsen, S. E. and Hansen, F.   1987   Measurements of the wind stress, heat flux and turbulence intensity during storm conditions over the North Sea. *J. Geophys. Res.*, **92**, 127–139

Grant, A. L. M.   1992   The structure of turbulence in the near-neutral atmospheric boundary layer. *J. Atmos. Sci.*, **49**, 226–239

Hare, J. E., Hara, T., Edson, J. B. and Wilczak, J. M.   1997   A similarity analysis of the structure of airflow over surface waves. *J. Phys. Oceanogr.*, **27**, 1018–1037

Högström, U.   1988   Non-dimensional wind and temperature profiles in the atmospheric surface layer: a re-evaluation. *Boundary-Layer Meteorol.*, **42**, 55–78

Højstrup, J.   1981   A simple model for the adjustment of velocity spectra in unstable conditions downstream of an abrupt change in roughness and heat flux. *Boundary-Layer Meteorol.*, **21**, 341–356

Højstrup, J., Edson, J., Hare, J., Courtney, M. S. and Sanderhoff, P.   1997   'The RASEX 1994 experiments'. Report R-788, Risø National Laboratory, Roskilde, Denmark

Howell, J. and Mahrt, L.   1997   Multiresolution flux decomposition. *Boundary-Layer Meteorol.*, **83**, 117–137

Howell, J. and Sun, J.   1999   Surface layer fluxes in stable conditions. *Boundary-Layer Meteorol.*, in press

Khanna, S. and Brasseur, J. G.   1997   Analysis of Monin–Obukhov similarity from large eddy simulation. *J. Fluid Mech.*, **345**, 251–286

Kitaigorodskii, S. A.   1970   *The physics of air–sea interaction.* Hydrometeorological Press, Lenningrad, Russia (English translation, 1973, available as TT 72-50062 from US National Technical Information Service, Springfield, VA 22151 USA)

Large, W. G., Morzel, J. and Crawford, G. B.   1995   Accounting for surface wave distortion of the marine wind profile in low-level ocean storms wind measurements. *J. Phys. Oceanogr.*, **25**, 2959–2971

Maat, N., Kraan, C. and Oost, W. A.   1991   The roughness of wind waves. *Boundary-Layer Meteorol.*, **54,** 89–103

Mahrt, L.   1998   Flux sampling errors for aircraft and towers. *J. Atmos. Oceanic Technol.*, **15,** 416–429

Mahrt, L., Vickers, D., Howell, J., Højstrup, J., Wilczak, J. A., Edson, J. and Hare , J.   1996   Sea surface drag coefficients in RASEX. *J. Geophys. Res.*, **101,** 14327–14335

Mahrt, L., Vickers, D., Edson, J., Sun, J., Højstrup, J., Hare, J. and Wilczak, J. A.   1998   Heat flux in the coastal zone. *Boundary-Layer Meteorol.*, **85,** 53–79

Makin, V. K., Kudryavtsev, V. N. and Mastenbroek, C.   1995   Drag of the sea surface. *Boundary-Layer Meteorol.*, **73,** 159–182

Miller, S., Friehe, C., Hristov, T., Edson, J. and Wetzel, S.   1997   'Wind and turbulence profiles in the surface layer over ocean waves'. Pp. 91–98 in Proceedings of the wind-over-wave couplings conference, University of Salford, April 1997. Eds. S. G. Sajjadi, N. H. Thomas and J. C. R. Hunt. Oxford University Press, New York, USA

Monin, A. S. and Obukhov, A. M.   1954   Basic laws of turbulent mixing in the atmosphere near the ground. *Tr. Akad. Nauk., SSSR Geophiz. Inst.*, No. 24 (151), 1963–1987

Nieuwstadt, F. T. M.   1984   The turbulent structure of the stable, nocturnal boundary layer. *J. Atmos. Sci.*, **41,** 2202–2216

Paulson, C. A.   1970   The mathematical representation of wind speed and temperature profiles in the unstable atmospheric surface layer. *J. Appl. Meteorol.*, **9,** 857–861

Peterson, E. W.   1969   Modification of mean flow and turbulent energy by a change in surface roughness under conditions of neutral stability. *Q. J. R. Meteorol. Soc.*, **95,** 561–575

Smedman, A. and Johansson, C.   1997   'Modifications of Monin–Obukhov similarity theory in unstable conditions'. Pp. 273–274 in Proceedings of the 12th Symposium on Boundary Layers and Turbulence, Vancouver. American Meteorological Society, Boston, USA

Smedman, A., Bergström, H. and Högström, U.   1995   Spectra, variance and length scales in a marine stable boundary layer dominated by a low level jet. *Boundary-Layer Meteorol.*, **76,** 211–232

Smith, S. D., Anderson, R. J., Oost, W. A., Kraan, C., Maat, N., DeCosmo, J., Katsaros, K. B., Davidson, K. L., Bumke, K., Hasse, L. and Chadwick, H. M.   1992   Sea surface wind stress and drag coefficients: the hexos results. *Boundary-Layer Meteorol.*, **60,** 109–142

Snyder, R. L., Dobson, F. W., Elliott, J. A. and Long, R. B.   1981   Array measurements of atmospheric pressure fluctuations above surface gravity waves. *J. Fluid Mech.*, **102,** 1–59

Sorbjan, Z.   1986   On similarity in the atmospheric boundary layer. *Boundary-Layer Meteorol.*, **34,** 377–397

Toba, Y. and Koga, M.   1986   A parameter describing overall conditions of wave breaking, white capping, sea-spray production and wind stress. Pp. 37–47 in *Oceanic whitecaps*. Eds. D. Reidel, E. C. Monahan and G. Mac Niocaill. D. Reidel Publishing Co., Dordrecht, the Netherlands

Vickers, D. and Mahrt, L.   1997a   Fetch limited drag coefficients. *Boundary-Layer Meteorol.*, **85,** 53–79

    1997b   Quality control and flux sampling problems for tower and aircraft data. *J. Atmos. Oceanic Technol.*, **14,** 512–526

Volkov, Y. A.   1970   Turbulent flux of momentum and heat in the atmospheric surface layer over disturbed sea surface. *Izv. Atmos. Oceanic Phys.*, **6,** 770–774

Wetzel, S. W., Edson, J. B., Friehe, C., Hristov, T. and Miller, S.   1996   'An investigation of wave-induced momentum flux through phase averaging of open ocean wind and wave fields'. Summary Report, Marine Boundary Layer, Accelerated Research Initiative Experiment Review, October 28–30 1996. Scripps Institution of Oceanography, La Jolla, CA, USA

Wyngaard, J. C.   1973   'On surface-layer turbulence'. Pp. 101–148 in Workshop on micrometeorology, Boston. Ed. D. A. Haugen. American Meteorological Society, Boston, USA